1521-0103/370/3/480–489$35.00
THE JOURNAL OF PHARMACOLOGY AND EXPERIMENTAL THERAPEUTICS

https://doi.org/10.1124/jpet.119.257501
J Pharmacol Exp Ther 370:480–489, September 2019

Activation of HIF-1α by δ-Opioid Receptors Induces COX-2 Expression in Breast Cancer Cells and Leads to Paracrine Activation of Vascular Endothelial Cells[S]

Alexandra Schoos, Cordula Gabriel, Vanessa M. Knab, and Daniela A. Fux

Division Clinical Pharmacology, Institute of Pharmacology and Toxicology (A.S., V.M.K., D.A.F.) and Institute of Pathology and Forensic Veterinary Medicine (C.G.), University of Veterinary Medicine Vienna, Vienna, Austria

Received February 14, 2019; accepted June 24, 2019

ABSTRACT

Opioids promote tumor angiogenesis in mammary malignancies, but the underlying signaling mechanism is largely unknown. The current study investigated the hypothesis that stimulation of δ-opioid receptors (DOR) in breast cancer (BCa) cells activates the hypoxia-inducible factor 1α (HIF-1α), which triggers synthesis and release of diverse angiogenic factors. Immunoblotting revealed that incubation of human MCF-7 and T47D breast cancer cells with the DOR agonist D-Ala^2,D-Leu^5-enkephalin (DADLE) resulted in a transient accumulation and thus activation of HIF-1α. DADLE-induced HIF-1α activation preceded PI3K/Akt stimulation and was blocked by the DOR antagonist naltrindole and naloxone, pertussis toxin, different phosphoinositide 3-kinase (PI3K) inhibitors, and the Akt inhibitor Akti-1/2. Whereas DADLE exposure had no effect on the expression and secretion of vascular endothelial growth factor (VEGF) in BCa cells, an increased abundance of cyclooxygenase-2 (COX-2) and release of prostaglandin E2 (PGE_2) was detected. DADLE-induced COX-2 expression was also observed in three-dimensional cultured MCF-7 cells and impaired by PI3K/Akt inhibitors and the HIF-1α inhibitor echinomycin. Supernatant from DADLE-treated MCF-7 cells triggered sprouting of endothelial (END) cells, which was blocked when MCF-7 cells were pretreated with echinomycin or the COX-2 inhibitor celecoxib. Also no sprouting was observed when END cells were exposed to the PGE_2 receptor antagonist PF-04418948. The findings together indicate that DOR stimulation in BCa cells leads to PI3K/Akt-dependent HIF-1α activation and COX-2 expression, which trigger END cell sprouting by paracrine activation of PGE_2 receptors. These findings provide a potential mechanism of opioid-driven tumor angiogenesis and thus therapeutic targets to combat the tumor-angiogenic opioid effect.

SIGNIFICANCE STATEMENT

Opioids are indispensable analgesics for treating cancer-related pain. However, opioids were found to promote tumor growth and metastasis, which questions the use of these potent pain-relieving drugs in cancer patients. Enhanced tumor vascularization after opioid treatment implies that tumor progression results from angiogenic opioid effects. Thus, understanding the signaling mechanism of opioid-driven tumor angiogenesis helps to identify therapeutic targets to combat these undesired tumor effects. The present study reveals that stimulation of δ-opioid receptors in breast cancer cells leads to an activation of HIF-1α and expression of COX-2 via PI3K/Akt stimulation, which results in a paracrine activation of vascular endothelial cells by prostaglandin E_2 receptors.

Introduction

Therapy of breast cancer is associated with pain in many ways. In addition to intra- and postoperative pain, pain caused by the tumor itself, by metastases, or by chemo- and radiotherapy requires the use of adequate analgesic drugs. For the relief of moderate and severe cancer pain, opioid analgesics are recommended (World Health Organization (WHO), 1996). However, there is growing evidence that the use of these potent analgesics is associated with adverse side effects in breast cancer patients. Different studies revealed that opioids may promote progression, metastasis, recurrence, growth, and angiogenesis of human mammary tumors (Gupta et al., 2002; Exadaktylos et al., 2006; Bimonte et al., 2015), and thus question the clinical use of opioids. As tumor angiogenesis—the formation of new vessels from the existing vasculature—contributes essentially to cancer growth and metastasis (Bielenberg and Zetter, 2015), understanding the still largely unknown mechanism of opioid-promoted vessel formation may help to find therapeutic targets to combat the tumor-supporting effects of opioids.

The hypoxia-inducible factor 1 (HIF-1) is a heterodimeric transcription factor, consisting of two subunits, HIF-1α and

https://doi.org/10.1124/jpet.119.257501.
[S] This article has supplemental material available at jpet.aspetjournals.org.

ABBREVIATIONS: BCa, breast cancer; CM, conditioned medium; CM^{cn}, conditioned medium from untreated MCF-7 cells; CM^{DADLE}, conditioned medium from DADLE-treated MCF-7 cells; COX-2, cyclooxygenase-2; 3D, three-dimensional; DADLE, D-Ala^2,D-Leu^5-enkephalin; DOR, δ-opioid receptors; END cells, endothelial cells; ER, estrogen receptor; FCS, fetal calf serum; GSK3, glycogen synthase kinase 3; HIF-1α, hypoxia-inducible factor 1α; IGF, insulin-like growth factor; MAPK, mitogen-activated protein kinase; OR, opioid receptor; PCR, polymerase chain reaction; PGE_2, prostaglandin E_2; PHD, prolyl hydroxylase domain; PI3K, phosphoinositide 3-kinase; PKA, protein kinase A; PTX, pertussis toxin; VEGF, vascular endothelial growth factor.

HIF-1β. Whereas HIF-1β is constitutively expressed, presence of HIF-1α is regulated by oxygen-sensitive prolyl hydroxylase domain enzymes (PHDs). In the presence of oxygen, HIF-1α is hydroxylated by PHDs and rapidly degraded by proteasomes (Huang et al., 1998; Schofield and Ratcliffe, 2004). At low oxygen concentrations (hypoxia), HIF-1α eludes from hydroxylation and degradation, translocates from the cytoplasm into the nucleus, and dimerizes with HIF-1β to gain full transcriptional activity (Dengler et al., 2014). HIF-1 regulates the expression of several proangiogenic factors, including the vascular endothelial growth factor VEGF-A (Krock et al., 2011), which is released as paracrine molecule to stimulate endothelial cell proliferation, migration, and tube formation (Hoeben et al., 2004). As HIF-1α knockout in breast cancer (BCa) cells significantly reduces VEGF expression and tumor vascularization (Schwab et al., 2012), HIF-1α is considered a key player in the process of breast cancer angiogenesis.

Oxygen-independent mechanisms may also stabilize and thus activate HIF-1α. In addition to inhibition of PHDs by cobalt chloride ($CoCl_2$) or desferrioxamine (Schofield and Ratcliffe, 2004), stimulation of receptor tyrosine kinases for the epidermal growth factor or insulin-like growth factor (IGF-1) (Zhong et al., 2000; Fukuda et al., 2002) as well as G protein-coupled thrombin and angiotensin II receptors has been shown to induce HIF-1α accumulation (Görlach et al., 2001; Pagé et al., 2002). Moreover, activation of phosphoinositide 3-kinase (PI3K)/Akt (Zundel et al., 2000) or cyclin-dependent kinase CDK1 (Warfel et al., 2013) allows HIF-1α activation by various stimuli under normoxic conditions.

Classic opioid effects such as analgesia, bradycardia, and constipation are mediated through the stimulation of μ-, δ-, or κ-opioid receptors (Connor and Christie, 1999; Kieffer and Evans, 2009; Pathan and Williams, 2012). Opioid receptors belong to the family of G protein-coupled receptors and trigger different signaling pathways, resulting in modulation of ion conductance, regulation of adenylyl cyclase activities, or stimulation of mitogen activated protein kinases (MAPK) (Al-Hasani and Bruchas, 2011). Opioid receptors are expressed in neuronal and diverse non-neuronal cells, including breast cancer cells and tissues (Zagon et al., 1987; Hatzoglou et al., 1996; Gach et al., 2011; Kharmate et al., 2013). A recent study showed that DOR expression in human breast tumors correlates with cancer stage, incidence of metastasis, and mortality rate (Wei et al., 2016), which implies a role of the opioid receptor type in mammary malignancies. In neuroblastoma × glioma NG108-15 hybrid cells, stimulation of DORs was shown to induce transactivation of IGF-1 receptors and PI3K/Akt activation (Heiss et al., 2009). Moreover, DOR stimulation in human heart tissue was found to trigger cellular effects that are similar to that induced by hypoxia (Bell et al., 2000). As hypoxia, IGF-1 receptor and PI3K/Akt signaling are closely related to HIF-1α activation, HIF-1α might represent a potential DOR downstream effector. To test the thesis, we examined here the effect of DOR stimulation on HIF-1α accumulation in human breast cancer cells and analyzed whether HIF-1α regulation may account for angiogenic opioid function.

Material and Methods

Cell Culture. Human breast cancer MCF-7 (ATCC HTB-22; American Type Culture Collection, Manassas, VA) and T47D cells (ATCC HTB-133) were cultured in Dulbecco's modified Eagle's medium (Sigma-Aldrich, St. Louis, MO) supplemented with 10% fetal calf serum (FCS; HyClone UK Ltd., Thermo Scientific, Northumberland, UK), 1% penicillin (100 U/ml), and 100 μg/ml streptomycin (Sigma-Aldrich). Cells were tested to be free of mycoplasma by polymerase chain reaction (PCR) using genus-specific primers according to Vojdani et al. (1998). Murine endothelial (END) cells (Gotthardt et al., 2016) were routinely grown in Roswell Park Memorial Institute medium (Sigma-Aldrich) supplemented with 10% FCS, 1% penicillin (100 U/ml), and 100 μg/ml streptomycin. All cells were cultured at 37°C in a humidified atmosphere in presence of 5% CO_2. For experiments, cells were grown in 6- (Falcon, Corning, NY) or 12-well culture plates (SPL Life Sciences Co. Ltd., Gyeonggi-do, Korea). For 3D cell culture, MCF-7 or END cells (10^5/ml) were seeded into nonadherent, U-bottom 96-well microtiter plates (BRAND GmbH & Co. KG, Wertheim, Germany) and cultured for 5 days in complete medium.

Cell Treatments. To test HIF-1α accumulation under normoxic conditions, MCF-7 and T47D cells were exposed to 100 μM cobalt chloride ($CoCl_2$; Sigma-Aldrich) or 1 μM [D-Ala^2,D-Leu^5]-enkephalin (DADLE) (Sigma-Aldrich). Activation of DORs was blocked by cell treatment with 10 μM naltrindole (Sigma-Aldrich) or 10 μM naloxone for 10 minutes prior to DADLE exposure. The role of $G_{i/o}$ proteins was examined by cell pretreatment with 100 ng/ml pertussis toxin (PTX; Thermo Fisher Scientific, Waltham, MA) for 18 hours. To analyze the role of Akt signaling, cells were pretreated with the Akt inhibitor Akti-1/2 (100 μM, 15 minutes; Selleckchem, Munich, Germany) or the PI3K inhibitors wortmannin (2.5 μM, 30 minutes; Sigma-Aldrich), LY294002 2-(4-Morpholinyl)-8-phenyl-1(4H)-benzopyran-4-one; 10 μM, 30 minutes; Sigma-Aldrich), BKM120 5-(2,6-dimorpholinopyrimidin-4-yl)-4-(trifluoromethyl)pyridin-2-amine; 1 μM, 10 minutes; Sigma-Aldrich), or BEZ235 (4-[2,3-dihydro-3-methyl-2-oxo-8-(3-quinolinyl)-1H-imidazo[4,5-c]quinolin-1-yl]-α,α-dimethyl-benzeneacetonitrile; 1 μM, 10 minutes; Sigma-Aldrich). To inhibit HIF-1α activity, cells were pretreated with 10 nM echinomycin (Calbiochem; EMD Chemicals, Inc., San Diego, CA) for 10 minutes. Celecoxib (50 μM; 30 minutes; Tocris Bioscience, Bio-Techne Ltd., Minneapolis, MN) was used to inhibit cyclooxygenase 2 (COX-2) activity, whereas prostaglandin E receptor was blocked by PF-04418948 (1-(4-fluorobenzoyl)-3-[[(6-methoxy-2-naphthalenyl)oxy]methyl]-3-azetidinecarboxylic acid; 10 μM, 30 minutes; Tocris Bioscience).

Western Blotting. MCF-7 and T47D cells were lysed by addition of Laemmli sample buffer (62.5 mM Tris-HCl, pH 6.8, 2% SDS, 50 mM DTT, 10% glycerol, 0.01% bromophenole blue), denaturated by 95°C for 5 minutes and subjected to sodium dodecyl sulfate polyacrylamide gel electrophoresis using 8% or 10% polyacrylamide gels. Proteins were transferred to a polyvinylidene fluoride membrane (PVDF Blotting-Membrane, peqlab; VWR International GmbH, Erlangen, Germany), which was subsequently blocked with 5% non-fat milk powder (Carl Roth GmbH + Co. KG, Karlsruhe, Germany) dissolved in Tris-buffered saline with 0.1% Tween-20 (TBST) for 60 minutes. Membranes were then incubated with rabbit monoclonal HIF-1α antibody [1:1000, Cat# 14179; Cell Signaling Technology (CST), Inc., Danvers, MA], rabbit monoclonal phospho-Serine-473-Akt antibody (1:1000, Cat #4060; CST), rabbit polyclonal Akt antibody (1:1000, Cat #9272; CST), rabbit monoclonal COX-2 antibody (1:1000, Cat# 12282; CST), or mouse monoclonal HSC70 antibody (1:1000, Cat# SC7298; Santa Cruz Biotechnology, Dallas, TX) at 4°C overnight. After being washed with TBST, membranes were incubated with horseradish-peroxidase conjugated anti-rabbit (Cat# 7074; Cell Signaling Technology) or anti-mouse IgG (Cat# 7076; Cell Signaling Technology) for 60 minutes at room temperature. Membranes were finally exposed to Clarity Western ECL Substrate (Bio-Rad Laboratories, Inc., Irvine, CA) and immunoreactivity was measured by chemiluminesence using Bio-Rad ChemiDoc Touch and Image Laboratory Software (Bio-Rad Laboratories, Inc.).

Real-Time Quantitative PCR. Total RNA was isolated using peqGOLD TriFast (VWR International GmbH, Life Science Competence Center, Darmstadt, Germany) according to the manufacturer's protocol. One microgram of total RNA was subjected to reverse

transcription using the iScript cDNA Synthesis Kit (Bio-Rad Laboratories, Inc.). Amplifications were run on a CFX96 Real-Time System C1000Touch Thermal Cycler (Bio-Rad Laboratories, Inc.) using SsoAdvanced Universal SYBR Green Supermix (Bio-Rad Laboratories, Inc.). Primers used were as follows: HPRT1 (reference gene #1: hypoxanthine phosphoribosyltransferase 1; NM_000194): forward 5′-ATGGACAGGACTGAACGTCTT-3′ and reverse 5′-TGG GGTCCTTTTCACCAGCA-3′, RPS18 (reference gene #2: ribosomal protein S18, NM_022551.2): forward 5′-ATTAAGGGTGTGGGCCGA AG-3′ and reverse 5′-TGGCTAGGACCTGGCTGTAT-3′, VEGF-A/total (NM_001025366.2), VEGF-A_{121} (NM_001025370.2), and VEGF-A_{165} NM_001287044.1): forward 5′-CCCTGATGAGATCGAGTACATC-3′ and reverse 5′-ACCGCCTCGGCTTGTCAC-3′ (VEGF-A/total), 5′-GCCTCGGCTTGTCACATTTTC-3′ (VEGF-A_{121}), and 5′-CAAGGC CCACAGGGATTTTC-3′ (VEGF-A_{165}). Controls without reverse transcription or without template cDNA were included in each assay. Results were normalized to reference genes HPRT1 and RPS18. Relative gene expression levels were obtained using the $\Delta\Delta C_q$ method (Livak and Schmittgen, 2001) and the Bio-Rad CFX Manager Software.,

Human Angiogenesis Array. MCF-7 and T47D cells were incubated with 1 μM DADLE for 24 hours in FCS-reduced medium. Cell culture supernatant was collected and analyzed for VEGF and other angiogenic factors by using Human Angiogenesis Array Kit (Cat# ARY007, Proteome Profiler Array; R&D Systems, Minneapolis, MN) according to manufacturers' instructions.

PGE_2 ELISA. MCF-7 and T47D cells were grown in a six-well plate and incubated with 1 μM DADLE for 24 hours. Cell culture supernatant was collected, cleared from cells by centrifugation, and stored at −20°C until being analyzed for PGE_2 concentrations. Quantification of PGE_2 was performed in duplicates from each sample by using the Prostaglandin E2 Parameter Assay Kit (Cat# KGE004B; R&D Systems) in accordance to the manufacturers' instruction. Absorbance was measured on an EnSpire Multiplate Reader (Perkin Elmer, Waltham, MA).

Immunohistochemistry. Three-dimensional cultured MCF-7 cells were exposed to 1 μM DADLE in presence and absence of BEZ235 or BKM120 for 3 hours, collected by centrifugation for 2 minutes at 2000 rpm, washed two times with Dulbecco's phosphate-buffered saline, fixed with 4% formaldehyde (48 hours; 4°C), and embedded in Paraplast medium (Vogel, Giessen, Germany). Serial sections of 3 μm thickness were cut and mounted on 3-aminopropyltriethoxysilane/glutaraldehyde-coated slides. After a drying period of 12 hours, sections were exposed to 0.6% H_2O_2 in methanol for 15 minutes at room temperature and incubated with 0.01 M citrate buffer (pH 6.0) for 30 minutes in a steamer for antigen retrieval. Sections were then washed with PBS for 5 minute, blocked with 1.5% normal goat serum (Sigma Aldrich) and incubated with rabbit monoclonal COX-2 antibody (1:500, CloneSP21, Cat# RM-9121; Thermo Fisher Scientific). Sections were washed and exposed to anti-rabbit poly-horseradish peroxidase secondary antibody (BrightVision Immunologic, Duiven, The Netherlands) and 3,3′diaminobenzidine-tetrahydrochloride substrate (Sigma Aldrich) solved in Tris-HCl buffer pH 7.4 and 0.03% H_2O_2 as chromogen. Finally, slides were washed with distilled water, counterstained with haemalum, dehydrated, and mounted by using xylene-soluble medium (DPX; Sigma Aldrich). Negative controls were performed by substitution of the primary antibody with PBS. Sections were examined using the Polyvar light microscope (Reichert-Jung, Vienna, Austria) with a digital DS-Fi1 camera (Nikon, Vienna, Austria) and Nikon NIS elements software.

Sprouting Assay. Five-day-old spheroids from murine END cells were transferred from nonadherent U-bottom to flat bottom 96-well plates coated with collagen I rat protein (1 mg/ml; Thermo Fisher Scientific) and exposed to supernatant collected from MCF-7 cells treated with 1 μM DADLE in presence or absence of indicated inhibitors for 24 hours. In a second approach, END cell spheroids were treated with PF-04418948 before being exposed to supernatant from DADLE-treated MCF-7 cells. END cell spheroids were cultured for 24 hours, photographed by using the Olympus IX71 microscope (Olympus K.K., Tokyo, Japan) with an Olympus DP72 camera (Olympus K.K.) and CellSens Dimension software (Olympus K.K.), and assessed for sprouting area by using Image J.

Data Analysis. Data are presented as mean ± S.E.M., and analyzed by using GraphPad Prism 5.0 for Windows (GraphPad Software Inc., La Jolla, CA). To assess statistical significance, an unpaired Student's *t*-test with Welch correction was used. A P value <0.05 was considered statistically significant.

Results

DADLE Induces HIF-1α in Human Breast Cancer Cells. The effect of DOR stimulation on HIF-1 α was examined in human MCF-7 and T47D breast cancer cells, which do endogenously express DORs (Kharmate et al., 2013). To evaluate whether DOR activation leads to HIF-1α activation, MCF-7 and T47D cells were exposed to 1 μM DADLE for 1–6 hours, and examined for HIF-1α protein by immunoblotting (Fig. 1A). As a positive control, cells were incubated with 100 μM $CoCl_2$ for 3 hours (Yuan et al., 2003). Compared with nontreated cells, incubation with $CoCl_2$ resulted in a prominent increase of HIF-1α in both BCa cell lines. Also cell exposure to 1 μM DADLE enhanced the amount of HIF-1α protein: an increase of HIF-1 α protein was observed after a 1-hour DADLE

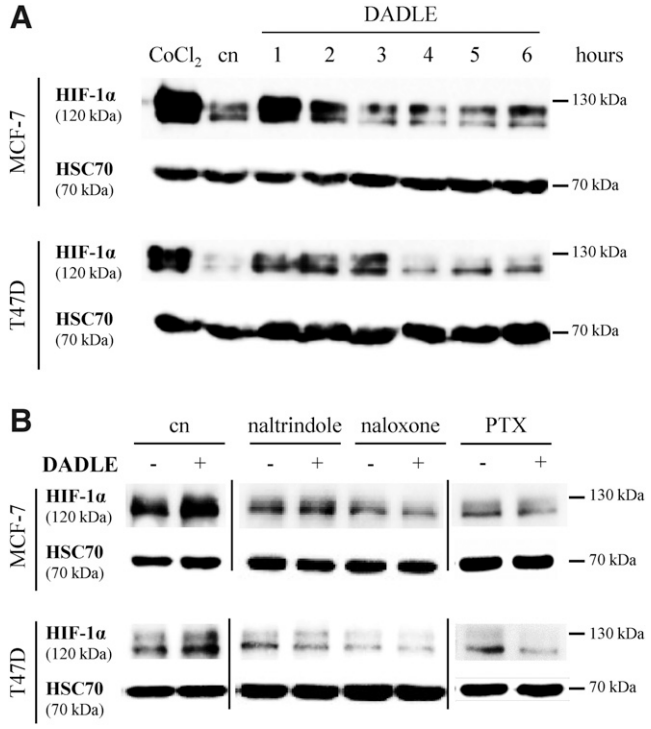

Fig. 1. HIF-1α accumulation in MCF-7 and T47D cells treated with DADLE. (A) MCF-7 and T47D cells were treated with 1 μM DADLE for 1–6 hours and examined for HIF-1α protein expression by immunoblotting. Controls (cn) were left untreated. Cells treated with 100 μM $CoCl_2$ for 3 hours were used as positive HIF-1α controls; HSC70 served as loading control. (B) Cells were pretreated with 10 μM naloxone or 10 μM naltrindole for 10 minutes or 100 ng/ml PTX for 18 hours followed by exposure to 1 μM DADLE for 1 hour. Controls (cn) were pretreated with sterile water as drug solvent control for 10 minutes. Subsequently, cells were lysed and examined for HIF-1α expression by immunoblotting. HSC70 served as loading control. Shown is one representative blot from three independent experiments (n = 3).

treatment in both BCa cell lines, which remained elevated for 2 hours in MCF-7 and 3 hours in T47D cells before returning back to basal levels. Pretreatment of BCa cells with 10 μM naltrindole or 10 μM naloxone prevented DADLE-mediated HIF-1α increase (Fig. 1B). Likewise, DADLE failed to enhance HIF-1α in cells treated with 100 ng/ml pertussis toxin (PTX; Fig. 1B).

Inhibition of PI3K/Akt Prevents DADLE-Induced HIF-1α Accumulation. HIF-1α may be induced by PI3K/Akt signaling under nonhypoxic conditions (Agani and Jiang, 2013). To determine whether the signaling mechanism may also account for DADLE-induced HIF-1α, MCF-7 and T47D cells were first tested for Akt activation upon DADLE treatment. Compared with nontreated controls, DADLE exposure for 5–15 minutes increased the amount of Ser-473 phosphorylated Akt in both BCa cell lines (Fig. 2A). Pretreatment of MCF-7 and T47D cells with the PI3K inhibitors wortmannin and LY294002, or with the Akt inhibitor Akti-1/2 prevented DADLE-mediated Akt phosphorylation (Fig. 2A). To evaluate the impact of DADLE-induced Akt regulation for HIF-1α, MCF-7 and T47D cells were pretreated with PI3K/Akt inhibitors and analyzed for HIF-1α after DADLE exposure for 1 hour. In presence of wortmannin, LY294002 and Akti-1/2, DADLE incubation failed to induce HIF-1α accumulation (Fig. 2B). Moreover, DADLE-triggered HIF-1α accumulation was abolished by the PI3K inhibitors BEZ235 or BKM120 (Fig. 2B).

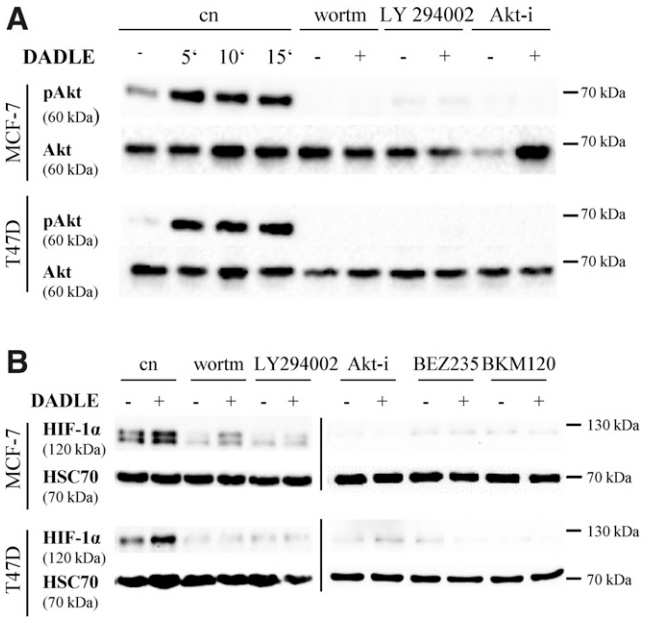

Fig. 2. Role of PI3K/Akt signaling in DADLE-regulated HIF-1α accumulation. (A) Akt activation by DADLE in breast cancer cells. MCF-7 and T47D cells were treated with 1 μM DADLE for indicated time periods. Cells pretreated with 2.5 μM wortmannin (30 minutes; wortm), 10 μM LY294002 (30 minutes), or 100 μM Akti-1/2 (15 minutes; Akt-i) were exposed to 1 μM DADLE for 10 minutes. Cells were lysed and subjected to Akt (Akt) and phospho-Serine-473-Akt (pAkt) analysis by immunoblotting. (B) HIF-1α accumulation is prevented by PI3K and Akt inhibitors. MCF-7 and T47D cells were pretreated with wortmannin (2.5 μM; 30 minutes; wortm), LY294002 (10 μM; 30 minutes), Akti-1/2 (100 μM; 15 minutes; Akt-i), BEZ235 (1 μM; 10 minutes), or BKM120 (1 μM; 10 minutes) and then exposed to 1 μM DADLE for 1 hour. Control cells (cn) were pretreated for 30 minutes with 1% DMSO as drug solvent control. Cell lysates were subjected to immunoblotting and probed for HIF-1α expression. HSC70 served as loading control. Shown is one representative immunoblot from three independent approaches ($n = 3$).

Effect of DADLE Treatment on VEGF Expression and Release. To investigate next whether DADLE-stimulated HIF-1α triggers the synthesis of angiogenic factors, MCF-7 and T47D cells were first analyzed for VEGF-A expression by real-time quantitative-PCR. As shown in Fig. 3A, incubation of BCa cells with 1 μM DADLE for 6 hours yielded similar amounts of VEGF-A mRNA as in the nontreated controls. Also, extended DADLE exposure for 12 or 24 hours had no effect on the abundance of VEGF-A mRNA (Fig. 3A). Likewise, the amount of mRNA of the VEGF-A splice variants VEGF-A_{121} and VEGF-A_{165} remained unaffected by DADLE treatment.

To evaluate whether DADLE treatment alters the release of VEGF, conditioned medium (CM) from MCF-7 and T47D cells cultured in the absence or presence of 1 μM DADLE for 24 hours were analyzed on an angiogenesis cytokine array. The analysis showed comparable amounts of VEGF in CM from DADLE-treated and nontreated BCa cells (Fig. 3B, red box). In addition, CM from BCa cells contained the proangiogenic factors CXCL16, angiogenin, amphiregulin, serpin E1 (only MCF-7 cells), urokinase plasminogen activator, IGFBP-2, IGFBP-3, and FGF-7 (only T47D cells), and the angiogenesis inhibitors TIMP-1 and thrombospondin (Fig. 3B). Neither qualitative nor quantitative differences were observed for these factors between CM from DADLE-treated and nontreated BCa cells.

DADLE Treatment Triggers COX-2 Expression and PGE_2 Release in Breast Cancer Cells. An alternative HIF-1α target with angiogenic function is COX-2 (Kaidi et al., 2006). Thus, MCF-7 and T47D cells were treated with 1 μM DADLE for 1–5 hours and analyzed next for COX-2 protein level by immunoblotting. Incubation of both BCa cell lines with DADLE for 1 hour increased the amount of COX-2 protein (Fig. 4A), which remained elevated for 4 hours in MCF-7 and 5 hours in T47D cells.

To further evaluate whether DADLE-induced COX-2 is functionally active, BCa cells were treated with 1 μM DADLE for 24 hours and tested for PGE_2 release by ELISA. Compared with CM collected from nontreated controls, the amount of PGE_2 was approximately two-times higher in CM from DADLE-treated MCF-7 and T47D cells (Fig. 4B). Pretreatment of BCa cells with the COX-2 inhibitor celecoxib (50 μM, 30 minutes) abolished the DADLE effect in both BCa cell lines. These findings demonstrate that DADLE treatment induced the expression of active COX-2 in MCF-7 and T47D cells.

Role of PI3K/Akt/HIF-1α Signaling in DADLE-Induced COX-2 Expression. To find out whether DADLE-mediated COX-2 expression is linked to PI3K/Akt-regulated HIF-1α, MCF-7, and T47D cells were pretreated with Akti-1/2, BEZ235, or BKM120 and subsequently examined for COX-2 protein level by immunoblotting. Pretreatment of MCF-7 cells with Akti-1/2 (100 μM, 15 minutes) or BEZ235 (1 μM; 10 minutes) enhanced basal level of COX-2 in MCF-7, but not in T47D cells (Fig. 5A). In contrast, incubation with BKM120 (1 μM, 10 minutes) had no effect on basal COX-2 expression. Cell exposure to 1 μM DADLE for 1 hour decreased protein level of COX-2 in MCF-7 cells pretreated with Akti-1/2 and BEZ-235, respectively. In MCF-7 cells pretreated with BKM120, DADLE had no effect on COX-2 protein level (Fig. 5A).

To examine the role of DADLE-induced HIF-1α, MCF-7, and T47D cells were exposed to echinomycin, which inhibits the

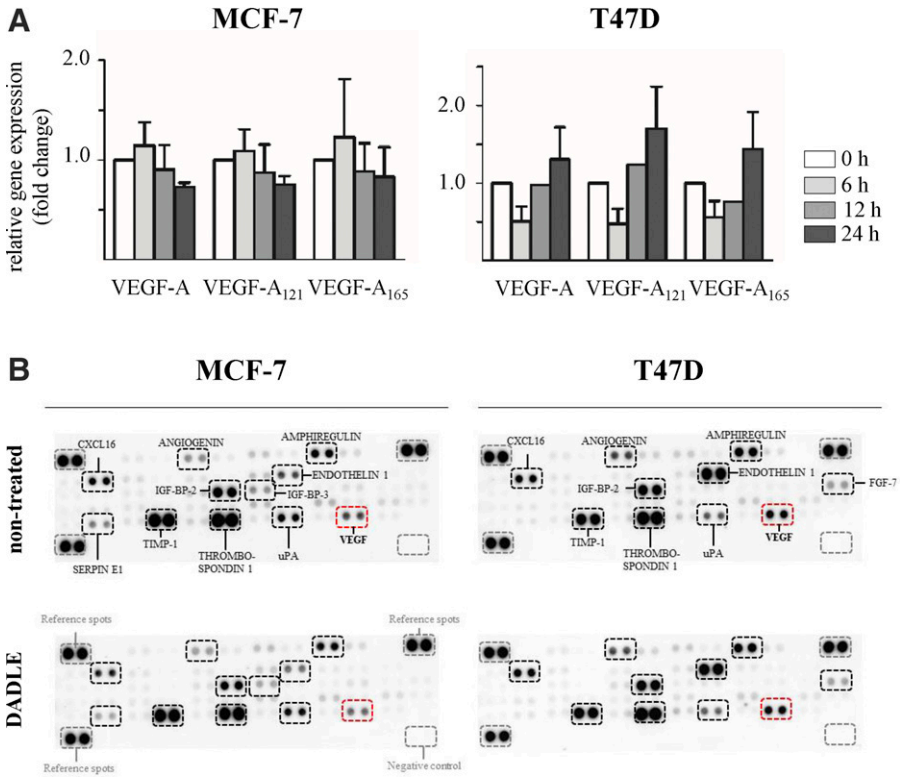

Fig. 3. Effect of DADLE treatment on VEGF expression and release. (A) VEGF expression. MCF-7 and T47D cells were incubated with 1 μM DADLE for 6, 12, or 24 hours and examined for VEGF-A (total), VEGF-A121, and VEGF-A165 mRNA by RT-qPCR. Data are expressed as relative changes compared with the nontreated, corresponding controls. Values are presented as mean ± S.E.M. of triplicates in two independent experiments. Differences were not statistically relevant. (B) Analysis of conditioned medium from MCF-7 and T47D cells for VEGF-A and alternative angiogenic factors. MCF-7 and T47D cells were treated with 1 μM DADLE for 24 hours. Control cells remained untreated. Conditioned medium was collected and subjected to an angiogenesis cytokine array. Shown is one representative array out of two independent approaches with comparable results (n = 2).

binding of HIF-1α to the DNA (Kong et al., 2005). Incubation of BCa cells with 10 nM echinomycin prevented DADLE-induced increase of COX-2 protein in MCF-7 and T47D cells (Fig. 5B).

Regulation of HIF-1α and COX-2 in 3D-Cultured MCF-7 Cells. Next, the effect of DADLE on HIF-1α and COX-2 was examined in MCF-7 cells grown as 3D culture. First, 3D-cultured MCF-7 cells were incubated with 1 μM DADLE for 3 or 6 hours and analyzed for HIF-1α protein level by immunoblotting. Nontreated controls exhibited a basal level of HIF-1α protein, which was further increased after DADLE exposure for 3 hours (Fig. 6A); 3D cultures incubated with DADLE for 6 hours exhibited similar HIF-1α protein levels than the nontreated controls. To assess COX-2 regulation, 3D-grown MCF-7 cells were treated with 1 μM DADLE for 3 hours and then subjected to immunohistochemical analysis. Nontreated 3D cultures showed no COX-2 staining, whereas clusters of COX-2-positive cells were observed after DADLE exposure (Fig. 6B). Three-dimensional cultures treated with 1 μM BEZ235 or 1 μM BKM120 alone displayed scattered COX-2-positive cells, which were totally abolished after DADLE treatment.

Conditioned Medium from DADLE-Stimulated MCF-7 Cells Stimulates END Cells. We finally asked whether DADLE-induced HIF-1α/COX-2 signaling in breast cancer cells has angiogenic function. To address the question, we isolated CM from MCF-7 cells treated with 1 μM DADLE for 24 hours (CM^{DADLE}) and used it for incubation of END cells spheroids (Fig. 7A). END cell spheroids exposed to CM^{DADLE} for 24 hours showed multiple sprouts, whereas END cells treated with CM from nontreated MCF-7 cells (CM^{cn}) remained in a round shape (Fig. 7B). No sprouts were observed when END cell spheroids were exposed directly to 1 μM DADLE for up to 5 days (Supplemental Fig. 1). Also END cell spheroids pretreated with the EP2 receptor inhibitor PF-04418948 showed no sprouting after incubation with CM^{DADLE} (Fig. 7, B and C). Likewise, CM from MCF-7 cells exposed to DADLE and celecoxib, DADLE and naloxone or naltrindole, or DADLE and echinomycin failed to bring about sprout formation (Fig. 7, B and C). Comparable sprouting activities were also observed for END cell spheroids after incubation with CM from T47D cells treated with DADLE and respective inhibitors (Supplemental Fig. 2).

Discussion

Opioids promote breast cancer angiogenesis by a largely unknown mechanism. Here we demonstrate that DADLE induces HIF-1α accumulation in human MCF-7 and T47D breast cancer cells via PI3K/Akt activation. We further show that DADLE treatment enhances COX-2, but not VEGF expression, which triggers paracrine activation of END cells.

MCF-7 and T47D cells are classic in vitro models to study human estrogen receptor (ER)-positive breast cancer (Comşa et al., 2015; Yu et al., 2017). Exposure to DADLE enhanced HIF-1α protein levels in both cell lines and was prevented by the nonselective opioid receptor antagonist naloxone (Satoh and Minami, 1995), the DOR-selective antagonist naltrindole (Portoghese et al., 1988), and the $G_{i/o}$ protein inhibitor PTX (Leaney and Tinker, 2000). Thus, HIF-1α regulation results from stimulation of $G_{i/o}$ protein-dependent signaling of DORs and is not a cell line-specific DADLE effect. HIF-1α regulation by DORs was also observed in a previous study where fentanyl induced HIF-1α in human SH-SY-5Y neuroblastoma cells (Daijo et al., 2011). This suggests HIF-1α is a DOR downstream target in different human cancer cells and probably also an effector molecule of other $G_{i/o}$ protein-coupled receptors.

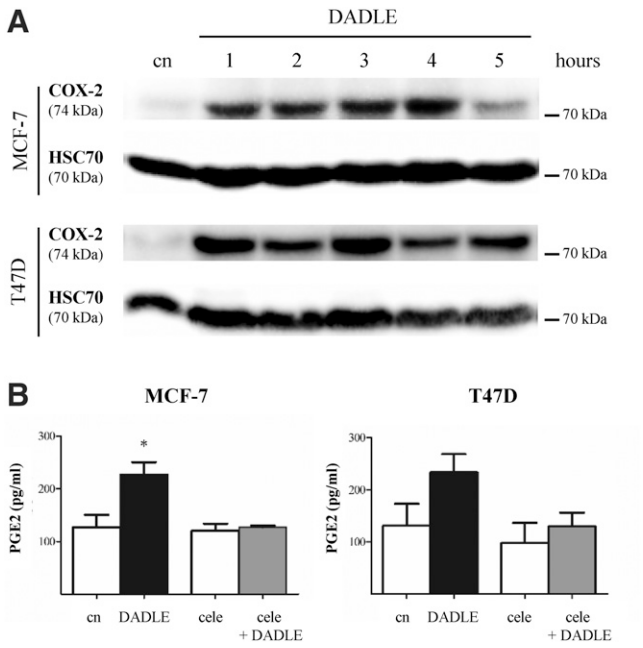

Fig. 4. DADLE stimulates COX-2 expression and PGE_2 release. (A) COX-2 expression in DADLE-treated MCF-7 and T47D cells. Cells were treated with 1 μM DADLE for 1–5 hours. Controls (cn) remained untreated. Cells were lysed and analyzed for COX-2 expression by immunoblotting. HSC70 served as loading control. Shown is one representative blot from three independent experiments ($n = 3$). (B) Analysis of PGE_2 released from DADLE-treated MCF-7 and T47D cells. MCF-7 and T47D cells were treated with 1 μM DADLE in presence or absence of 50 μM celecoxib (cele). After 24 hours, conditioned medium was collected and tested for PGE_2 concentration (pg/ml) by ELISA. Data represent mean ± S.E.M. from three individual experiments ($n = 3$). $^*P < 0.05$ compared with non-treated control (cn) by unpaired Welch's t test.

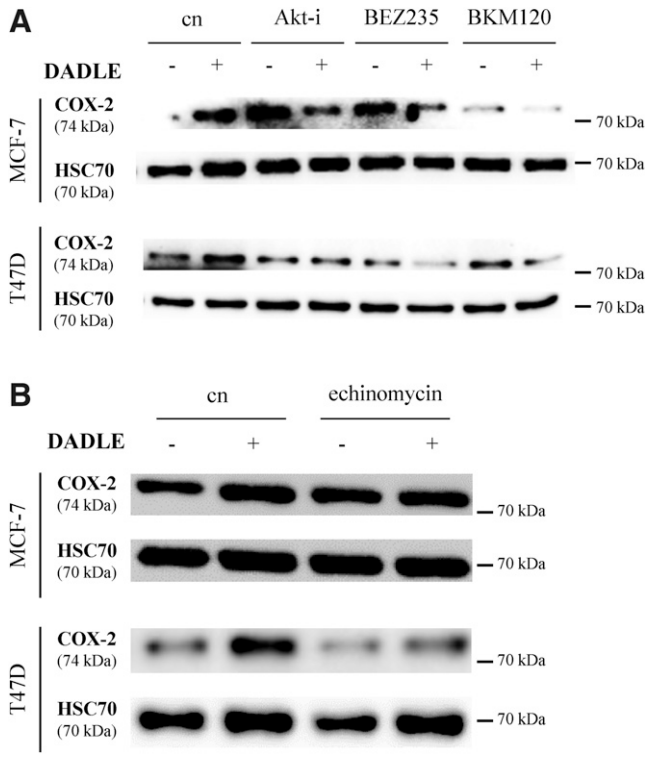

Fig. 5. Role of PI3K/Akt and HIF-1α in DADLE-mediated COX-2 expression. (A) Effect of PI3K and Akt inhibitors on COX-2 expression. MCF-7 and T47D cells were treated with 100 μM Akti-1/2 (15 minutes; Akt-i), 1 μM BEZ235 (10 minutes), or 1 μM BKM120 (10 minutes) before exposure to 1 μM DADLE for 1 hour. Controls (cn) were pretreated with 1% DMSO as solvent control. HSC70 served as loading control. Shown is one representative blot from three independent experiments $n = 3$. (B) Echinomycin blocks DADLE-induced COX-2 expression. MCF-7 and T47D cells were pretreated with 10 nM echinomycin for 10 minutes; controls (cn) remained untreated. After incubation with 1 μM DADLE for 1 hour, cells were lysed and tested for COX-2 protein by Western blotting. HSC70 served as loading control. Shown is one representative immunoblot from three independent experiments ($n = 3$).

DADLE induced a transient HIF-1α accumulation within 1 hour in MCF-7 and T47D cells. The fast onset is in large contrast to fentanyl-induced HIF-1α accumulation in SH-SY-5Y cells, which is observed only after 24 hours (Daijo et al., 2011). The fast kinetic in BCa cells suggests a direct DOR-mediated signaling mechanism, which allows HIF-1α induction by DADLE. Transient HIF-1α stimulation further implies that this signaling mechanism is terminated within 2 to 3 hours. It has been shown that stimulation of DORs by DADLE induces receptor desensitization, internalization, and subsequent degradation with comparable kinetics (Cvejic et al., 1996; Yoon et al., 1998; Eisinger et al., 2002). As these processes terminate DOR signaling, rate of DADLE-induced DOR internalization and degradation might account for transient HIF-1α accumulation in BCa cells.

DADLE treatment induced Akt activation in MCF-7 and T47D cells as indicated by Akt Ser-473 phosphorylation (Alessi et al., 1996). Inhibition of Akt phosphorylation by wortmannin and LY294002, two structurally unrelated PI3K inhibitors (Powis et al., 1994; Vlahos et al., 1994), confirms that DADLE-mediated Akt activation depends on PI3K in BCa cells as previously shown in NG108-15 cells (Heiss et al., 2009). Inhibition of HIF-1α induction by wortmannin and LY294002, but also BEZ235 and BKM120, two alternative PI3K inhibitors (Martín et al., 2017; Rodon et al., 2018), and Akti-1/2 revealed that the highly conserved PI3K/Akt pathway triggers HIF-1α accumulation by DADLE. PI3K/Akt signaling was postulated to stimulate *HIF-1α* gene transcription and translation and prevents HIF-1α protein degradation under normoxic conditions (Kietzmann et al., 2016; Iommarini et al., 2017). Although it is yet not clear which of these mechanisms account for DOR-induced HIF-1α, PI3K/Akt turned out to be the central driver and thus a potential target to interfere with DADLE-induced HIF-1α.

Although VEGF expression is a central response of HIF-1α activation (Forsythe et al., 1996), DADLE had no effect on transcription of VEGF-A including its most common isoforms, $VEGF\text{-}A_{121}$ and $VEGF\text{-}A_{165}$, or its secretion as indicated by the unchanged amount of VEGF peptide in the supernatant of treated and nontreated cells. Likewise, the release of CXCL16, Serpin E1, endothelin 1, and FGF-7 was unaffected. Interestingly, these paracrine factors are alternative HIF-1α targets (Yamashita et al., 2001; Chaturvedi et al., 2014; Rouillard et al., 2016), which let us suppose that DADLE-induced HIF-1α is either 1) transcriptionally inactive, 2) not sufficient to trigger expression and secretion of these angiogenic factors in detectable amounts, or 3) covered by other signaling mechanisms, which allow constitutive expression and release of these factors in MCF-7 and T47D cells. MCF-7 and T47D cells are characterized by the expression of ER and amplification of PKCα and RAF-1 (Shadeo and Lam, 2006). RAF-1 signaling induces endothelin-1 expression (Cheng et al., 2001), whereas

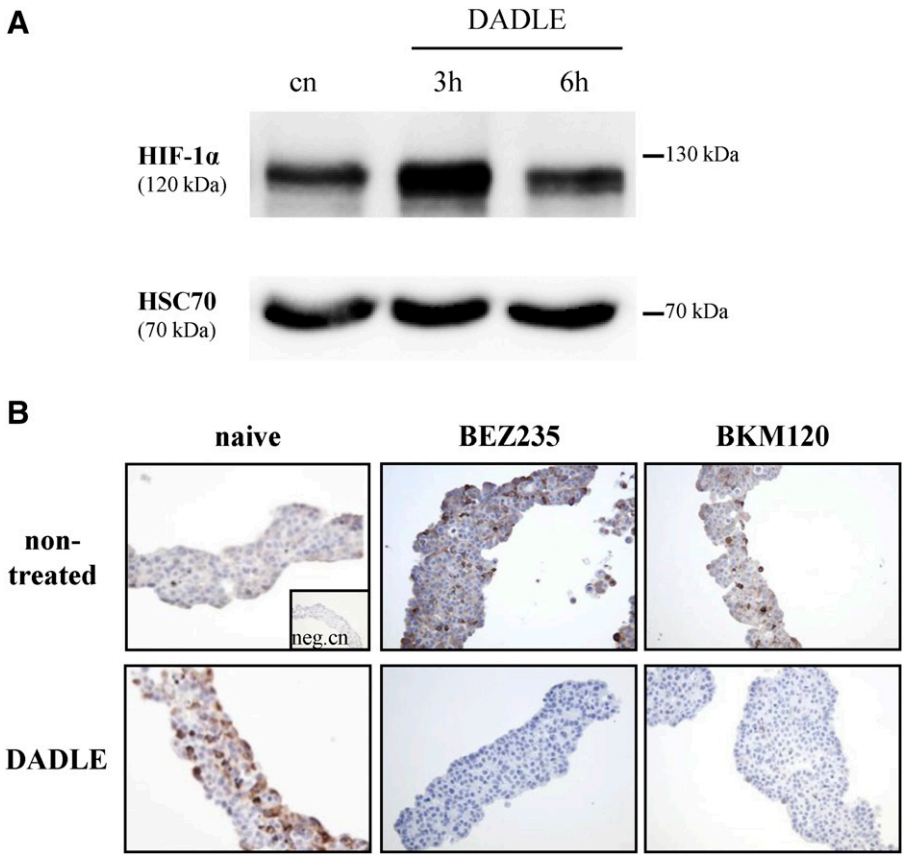

Fig. 6. Effect of DADLE treatment on HIF-1α and COX-2 expression in 3D-grown MCF-7 cells. (A) HIF-1α regulation. MCF-7 cells were grown as 3D culture, exposed to 1 μM DADLE for 3 or 6 hours and subjected to HIF-1α analysis by Western blotting. Controls (cn) were left untreated. HSC70 served as loading control. Shown immunoblots represent HIF-1α level from treated and untreated 3D-cultured MCF-7 cells, respectively (n = 24). Experiment was repeated three times with similar results. (B) Immunohistochemical staining of COX-2 in 3D cultured MCF-7 cells. 3D-cultured MCF-7 cells were pretreated with 1 μM BEZ235 or 1 μM BKM120 for 30 minutes followed by DADLE exposure for 3 hours. COX-2 expression was subsequently analyzed by immunohistochemistry. Representative images of corresponding 3D cultures from three independent experiments are shown. Insert shows the secondary antibody only control of IHC staining (neg.cn).

PKCα may promote CXCL16 release by ADAM10 activation (Gough et al., 2004; Kohutek et al., 2009). Moreover, activation of ER leads to the expression of VEGF, Serpin E1, and FGF-7 by HIF-1α-independent mechanisms (Ruohola et al., 1999; Smith et al., 2002; Gopal et al., 2012). As our experiments were conducted with medium containing phenol red, which has estrogen activity (Berthois et al., 1986), regulation of these pro-angiogenic factors by DADLE might be covered by the signaling of amplified RAF-1 and PKCα and ER activation in MCF-7 and T47D cells.

In contrast to VEGF, DADLE triggered the expression of catalytically active COX-2 in BCa cells. The ability of opioids to induce COX-2 upregulation has been already observed in vivo. Morphine treatment enhanced the content of COX-2 protein and PGE_2 in mammary tumors in mice (Farooqui et al., 2007), whereas the DOR selective agonist BW373U86 (±)-[1(S*),2α,5β]-4-[[2,5-Dimethyl-4-(2-propenyl)-1-piperazinyl](3-hydroxyphenyl)methyl]-N,N-diethylbenzamide upregulates the expression and activity of COX-2 in the myocardium (Kodani et al., 2002). The in vivo mechanism of opioid-induced COX-2 expression was not further examined. Inhibition of DADLE-induced COX-2 expression by echinomycin, BEZ235, and Akti-1/2 implicates a functional role for PI3K/Akt/HIF-1α signaling in BCa cells. As activation of HIF-1α or PI3K/Akt is associated with COX-2 upregulation in tumor cells (Kaidi et al., 2006; Xia et al., 2010), DADLE-induced PI3K/Akt/HIF-1α signaling is a plausible mechanism for COX-2 expression in BCa cells.

Considering that activation of PI3K/Akt enhances COX-2 expression in tumor cells (St.-Germain et al., 2004; Xia et al., 2010), it was surprising that incubation of BCa cells with the PI3K/Akt inhibitors Akti-1/2 and BEZ235 had the same effect. Interestingly, subsequent DADLE exposure suppressed Akti-1/2 and BEZ235-induced COX-2 expression. As the phenomenon was observed in MCF-7, but not T47D cells, a cell-type specific mechanism seems to trigger COX-2 upregulation after PI3K/Akt inhibition. Enhanced expression of COX-2 after PI3K/Akt inhibition by BEZ235 or Akt inhibitor X was previously observed for microglia (de Oliveira et al., 2012). The effect was suggested to result from an enhanced activity of glycogen synthase kinase 3 (GSK3), which is negatively regulated by PI3K/Akt (Jope et al., 2007). Considering the "GSK3 hypothesis," our observation implies that DOR signaling may block BEZ235 and Akti-1/2 induced GSK3 activity by a PI3K/Akt-independent mechanism. The activity of GSK3 is not only controlled by Akt (Cross et al., 1995). Also protein kinase A (PKA) terminates GSK3 activity (Fang et al., 2000). Zhang et al. (1999) showed that activation of p38 MAPK by DORs requires PKA activity, which implies that cAMP-dependent PKA may be stimulated by DORs. The mechanism of PKA activation by the opioid receptor has not been investigated so far, but studies revealed several signaling processes, by which $G_{i/o}$ protein-coupled receptors may stimulate PKA. For instance, PKA may be activated by cAMP produced by adenylyl cyclase 2 (AC2), AC4, and AC7, which are stimulated by G$\beta\gamma$ subunit (Khan et al., 2013). Alternatively, PKA is activated by $G_{i/o}$ coupled receptors as a result of IkB degradation upon stimulation of protein kinase C or JNK (Dulin et al., 2001). As DORs can activate AC2, PKC, and JNK (Ho et al., 1999; Kam et al., 2003; Eisinger and Ammer, 2008), several possibilities may be suggested for the signaling cascades leading to DADLE-induced activation of PKA. Independent of the underlying mechanism,

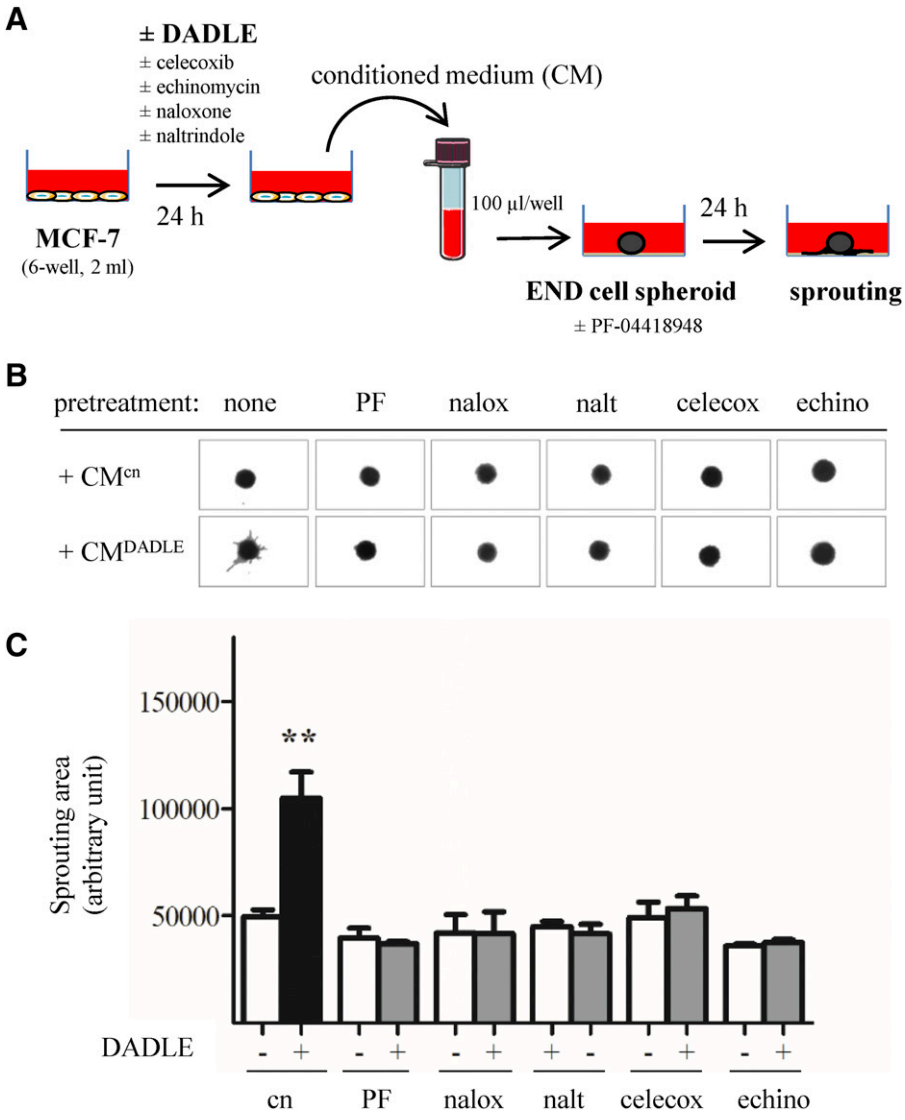

Fig. 7. Conditioned medium from DADLE-treated MCF-7 cells triggers sprouting of endothelial cells. (A) Experimental setup. MCF-7 cells were grown as monolayer in a six-well plate filled with 2 ml medium/well and treated with 1 μM DADLE in presence or absence of 50 μM celecoxib (30 minutes), 10 μM naloxone, 10 μM naltrindole, or 10 nM echinomycin (10 minutes) for 24 hours. Subsequently, 1.5 ml culture supernatant was collected and transferred to END cell spheroids placed on a collagen-coated 96-well plate (100 μl/well). After incubation for 24 hours, spheroids were analyzed for sprouting. (B) END cell sprouting. END cells were exposed to CM obtained from MCF-7 cells treated with 1 μM DADLE alone (CM^{DADLE}) or together with 10 nM echinomycin (echino), 10 μM naloxone (nalox), 10 μM naltrindole (nalt), or 50 μM celecoxib (celecox). CM collected from nontreated MCF-7 served as control (CM^{cn}). In addition, END cells were treated with 10 μM PF-04418948 (+PF) for 30 minutes before being exposed to CM^{DADLE}. Pictures show representatives END cell spheroids from each treatment group after 24-hour incubation. (C) Quantification of sprouting areas. Sprouting area was determined from 6 to 15 randomly selected spheroids per experimental group from three independent experiments and presented as mean ± S.E.M. $^{**}P < 0.05$ compared with CM^{cn} by unpaired Welch's t test.

PKA activation by DORs might thus suppress BEZ235- and Akti-1/2-induced COX-2 expression by GSK3 inhibition.

Studies have shown that findings from two-dimensional (2D, monolayer) cultured tumor cells differ from in vivo observations (Horman, 2016). Especially drug-induced regulation of HIF-1α observed in cell culture experiments has to be considered critical as solid tumors are often exposed to hypoxia and thus already feature HIF-1α overexpression (Zhong et al., 1999; Yang et al., 2017). To assess the biologic relevance of in vitro data, testing drug effects in 3D-cultured cells is state-of-the-art in cancer research, because 3D-cultured cells have similar characteristics as in vivo and are considered in vitro microtumor models (Ivascu and Kubbies, 2006). 3D-cultured cells also feature in vivo like oxygen gradients and HIF-1α expression (Chandrasekharan et al., 2002; Riedl et al., 2017), which render the models ideal tools to examine the effect of DADLE under tumor-like conditions. We used 3D-cultured MCF-7 cells, which exhibited a basal level of HIF-1α expression referring to hypoxic conditions in the microtumor model. Also, 3D-cultured MCF-7 cells showed transient increase of HIF-1α and COX-2 expression in response to DADLE treatment. Enhanced COX-2 expression after exposure to PI3K inhibitors and its inhibition by DADLE was observed as well. These findings indicates that DADLE-induced PI3K/HIF-1α/COX-2 signaling axis is not an artifact of 2D-cultured BCa cells but also occurs in microtumors under in vivo-like conditions.

COX-2 has a pivotal role in breast cancer progression (Rozic et al., 2001). Beside growth and metastasis, COX-2 expression is closely related to vascularization of mammary malignancies (Davies et al., 2003; Wang and DuBois, 2004). COX-2 activity was also revealed to promote morphine-mediated angiogenesis in a murine breast cancer model (Farooqui et al., 2007), which suggest DOR-induced PI3K/Akt/HIF-1α/COX-2 signaling in BCa cells a potential mechanism of angiogenic opioid effect. Findings from our END cell sprouting assay support the hypothesis and further suggest a paracrine mechanism underlying opioid-induced angiogenesis. We showed that conditioned medium from DADLE-treated MCF-7 and T47D cells, but not direct incubation with the opioid triggered END cell sprouting. We further showed that exposure of BCa cells to naloxone, naltrindole, celecoxib, and echinomycin prevented END cell sprouting by CM^{DADLE}, which indicates that DADLE-stimulated DORs induce the release of HIF-1α/COX-2 regulated factors with angiogenic properties. These paracrine

factors mediate END cell sprouting by the PGE_2 receptor EP2, as the EP2 receptor antagonist PF-04418948 blocked sprout formation. Stimulation of endothelial EP2 receptors has a central role in tumor angiogenesis (Kamiyama et al., 2006), so that paracrine activation by BCa cells in consequence of HIF-1α/COX-2 upregulation represents a possible mechanism of opioid-induced angiogenesis.

In summary, the present data elucidate that DOR stimulation in ER-positive BCa cells induces PI3K/Akt/HIF-1α/COX-2 signaling, resulting in paracrine activation of endothelial cells via EP2 receptor activation. It remains to be investigated whether the signaling mechanism also applies to other cancer cells expressing DORs, which would render opioid-induced tumor angiogenesis a much more widespread phenomenon in cancer patients. As PI3K inhibitors like BEZ235 and BKM120 are promising anticancer drugs in clinical trials (Martín et al., 2017; Rodon et al., 2018), targeting PI3K/Akt signaling represents a potential therapeutic strategy to combat the proangiogenic opioid effect.

Acknowledgments

The authors thank Felix Holstein and Claudia Höchsmann for technical support.

Authorship Contributions

Participated in research design: Fux.

Conducted experiments: Schoos, Knab, Gabriel, Fux.

Performed data analysis: Schoos, Gabriel, Fux.

Wrote or contributed to the writing of the manuscript: Schoos, Gabriel, Knab, Fux.

References

Agani F and Jiang BH (2013) Oxygen-independent regulation of HIF-1: novel involvement of PI3K/AKT/mTOR pathway in cancer. *Curr Cancer Drug Targets* **13**: 245–251.

Alessi DR, Andjelkovic M, Caudwell B, Cron P, Morrice N, Cohen P, and Hemmings BA (1996) Mechanism of activation of protein kinase B by insulin and IGF-1. *EMBO J* **15**:6541–6551.

Al-Hasani R and Bruchas MR (2011) Molecular mechanisms of opioid receptor-dependent signaling and behavior. *Anesthesiology* **115**:1363–1381.

Bell SP, Sack MN, Patel A, Opie LH, and Yellon DM (2000) Delta opioid receptor stimulation mimics ischemic preconditioning in human heart muscle. *J Am Coll Cardiol* **36**:2296–2302.

Berthois Y, Katzenellenbogen JA, and Katzenellenbogen BS (1986) Phenol red in tissue culture media is a weak estrogen: implications concerning the study of estrogen-responsive cells in culture. *Proc Natl Acad Sci USA* **83**:2496–2500.

Bielenberg DR and Zetter BR (2015) The contribution of angiogenesis to the process of metastasis. *Cancer J* **21**:267–273.

Bimonte S, Barbieri A, Rea D, Palma G, Luciano A, Cuomo A, Arra C, and Izzo F (2015) Morphine promotes tumor angiogenesis and increases breast cancer progression. *BioMed Res Int* **2015**:161508.

Chandrasekharan NV, Dai H, Roos KLT, Evanson NK, Tomsik J, Elton TS, and Simmons DL (2002) COX-3, a cyclooxygenase-1 variant inhibited by acetaminophen and other analgesic/antipyretic drugs: cloning, structure, and expression. *Proc Natl Acad Sci USA* **99**:13926–13931.

Chaturvedi P, Gilkes DM, Takano N, and Semenza GL (2014) Hypoxia-inducible factor-dependent signaling between triple-negative breast cancer cells and mesenchymal stem cells promotes macrophage recruitment. *Proc Natl Acad Sci USA* **111**:E2120–E2129.

Cheng TH, Shih NL, Chen SY, Loh SH, Cheng PY, Tsai CS, Liu SH, Wang DL, and Chen JJ (2001) Reactive oxygen species mediate cyclic strain-induced endothelin-1 gene expression via Ras/Raf/extracellular signal-regulated kinase pathway in endothelial cells. *J Mol Cell Cardiol* **33**:1805–1814.

Comşa Ş, Cîmpean AM, and Raica M (2015) The story of MCF-7 breast cancer cell line: 40 years of experience in research. *Anticancer Res* **3154**:3147–3154.

Connor M and Christie MD (1999) Opioid receptor signalling mechanisms. *Clin Exp Pharmacol Physiol* **26**:493–499.

Cross DA, Alessi DR, Cohen P, Andjelkovich M, and Hemmings BA (1995) Inhibition of glycogen synthase kinase-3 by insulin mediated by protein kinase B. *Nature* **378**: 785–789.

Cvejic S, Trapaidze N, Cyr C, and Devi LA (1996) Thr353, located within the COOH-terminal tail of the δ opiate receptor, is involved in receptor down-regulation. *J Biol Chem* **271**:4073–4076.

Daijo H, Kai S, Tanaka T, Wakamatsu T, Kishimoto S, Suzuki K, Harada H, Takabuchi S, Adachi T, Fukuda K, et al. (2011) Fentanyl activates hypoxia-inducible factor 1 in neuronal SH-SY5Y cells and mice under non-hypoxic conditions in a μ-opioid receptor-dependent manner. *Eur J Pharmacol* **667**: 144–152.

Davies G, Salter J, Hills M, Martin LA, Sacks N, and Dowsett M (2003) Correlation between cyclooxygenase-2 expression and angiogenesis in human breast cancer. *Clin Cancer Res* **9**:2651–2656.

Dengler VL, Galbraith M, and Espinosa JM (2014) Transcriptional regulation by hypoxia inducible factors. *Crit Rev Biochem Mol Biol* **49**:1–15.

de Oliveira AC, Candelario-Jalil E, Langbein J, Wendeburg L, Bhatia HS, Schlachetzki JC, Biber K, and Fiebich BL (2012) Pharmacological inhibition of Akt and downstream pathways modulates the expression of COX-2 and mPGES-1 in activated microglia. *J Neuroinflammation* **9**:2.

Dulin NO, Niu J, Browning DD, Ye RD, and Voyno-Yasenetskaya T (2001) Cyclic AMP-independent activation of protein kinase A by vasoactive peptides. *J Biol Chem* **276**:20827–20830.

Eisinger DA and Ammer H (2008) Delta-opioid receptors activate ERK/MAP kinase via integrin-stimulated receptor tyrosine kinases. *Cell Signal* **20**:2324–2331.

Eisinger DA, Ammer H, and Schulz R (2002) Chronic morphine treatment inhibits opioid receptor desensitization and internalization. *J Neurosci* **22**:10192–10200.

Exadaktylos AK, Buggy DJ, Moriarty DC, Mascha E, and Sessler DI (2006) Can anesthetic technique for primary breast cancer surgery affect recurrence or metastasis? *Anesthesiology* **105**:660–664.

Fang X, Yu SX, Lu Y, Bast RC Jr, Woodgett JR, and Mills GB (2000) Phosphorylation and inactivation of glycogen synthase kinase 3 by protein kinase A. *Proc Natl Acad Sci USA* **97**:11960–11965.

Farooqui M, Li Y, Rogers T, Poonawala T, Griffin RJ, Song CW, and Gupta K (2007) COX-2 inhibitor celecoxib prevents chronic morphine-induced promotion of angiogenesis, tumour growth, metastasis and mortality, without compromising analgesia. *Br J Cancer* **97**:1523–1531.

Forsythe JA, Jiang BH, Iyer NV, Agani F, Leung SW, Koos RD, and Semenza GL (1996) Activation of vascular endothelial growth factor gene transcription by hypoxia-inducible factor. *Mol Cell Biol* **16**:4604–4613.

Fukuda R, Hirota K, Fan F, Jung YD, Ellis LM, and Semenza GL (2002) Insulin-like growth factor 1 induces hypoxia-inducible factor 1-mediated vascular endothelial growth factor expression, which is dependent on MAP kinase and phosphatidylinositol 3-kinase signaling in colon cancer cells. *J Biol Chem* **277**:38205–38211.

Gach K, Szemraj J, Wyrębska A, and Janecka A (2011) The influence of opioids on matrix metalloproteinase-2 and -9 secretion and mRNA levels in MCF-7 breast cancer cell line. *Mol Biol Rep* **38**:1231–1236.

Gopal S, Garibaldi S, Goglia L, Polak K, Palla G, Spina S, Genazzani AR, Genazzani AD, and Simoncini T (2012) Estrogen regulates endothelial migration via plasminogen activator inhibitor (PAI-1). *Mol Hum Reprod* **18**:410–416.

Görlach A, Diebold I, Schini-Kerth VB, Berchner-Pfannschmidt U, Roth U, Brandes RP, Kietzmann T, and Busse R (2001) Thrombin activates the hypoxia-inducible factor-1 signaling pathway in vascular smooth muscle cells: role of the p22(phox)-containing NADPH oxidase. *Circ Res* **89**:47–54.

Gotthardt D, Putz EM, Grundschober E, Prchal-Murphy M, Straka E, Kudweis P, Heller G, Bago-Horvath Z, Witalisz-Siepracka A, Cumaraswamy AA, et al. (2016) STAT5 is a key regulator in NK cells and acts as a molecular switch from tumor surveillance to tumor promotion. *Cancer Discov* **6**:414–429.

Gough PJ, Garton KJ, Wille PT, Rychlewski M, Dempsey PJ, and Raines EW (2004) A disintegrin and metalloproteinase 10-mediated cleavage and shedding regulates the cell surface expression of CXC chemokine ligand 16. *J Immunol* **172**: 3678–3685.

Gupta K, Kshirsagar S, Chang L, Schwartz R, Law PY, Yee D, and Hebbel RP (2002) Morphine stimulates angiogenesis by activating proangiogenic and survival-promoting signaling and promotes breast tumor growth. *Cancer Res* **62**:4491–4498.

Hatzoglou A, Bakogeorgou E, and Castanas E (1996) The antiproliferative effect of opioid receptor agonists on the T47D human breast cancer cell line, is partially mediated through opioid receptors. *Eur J Pharmacol* **296**:199–207.

Heiss A, Ammer H, and Eisinger DA (2009) delta-Opioid receptor-stimulated Akt signaling in neuroblastoma x glioma (NG108-15) hybrid cells involves receptor tyrosine kinase-mediated PI3K activation. *Exp Cell Res* **315**:2115–2125.

Ho MKC, Yung LY, and Wong YH (1999) Disruption of receptor-mediated activation of G protein by mutating a conserved arginine residue in the switch II region of the alpha subunit. *J Neurochem* **73**:2101–2109.

Hoeben A, Landuyt B, Highley MS, Wildiers H, Van Oosterom AT, and De Bruijn EA (2004) Vascular endothelial growth factor and angiogenesis. *Pharmacol Rev* **56**: 549–580.

Horman SR (2016) Complex High-Content Phenotypic Screening, *Special Topics in Drug Discovery*, InTech.

Huang LE, Gu J, Schau M, and Bunn HF (1998) Regulation of hypoxia-inducible factor 1alpha is mediated by an O2-dependent degradation domain via the ubiquitin-proteasome pathway. *Proc Natl Acad Sci USA* **95**:7987–7992.

Iommarini L, Porcelli AM, Gasparre G, and Kurelac I (2017) Non-canonical mechanisms regulating hypoxia-inducible factor 1 alpha in cancer. *Front Oncol* **7**:286.

Ivascu A and Kubbies M (2006) Rapid generation of single-tumor spheroids for high-throughput cell function and toxicity analysis. *J Biomol Screen* **11**:922–932.

Jope RS, Yuskaitis CJ, and Beurel E (2007) Glycogen synthase kinase-3 (GSK3): inflammation, diseases, and therapeutics. *Neurochem Res* **32**:577–595.

Kaidi A, Qualtrough D, Williams AC, and Paraskeva C (2006) Direct transcriptional up-regulation of cyclooxygenase-2 by hypoxia-inducible factor (HIF)-1 promotes colorectal tumor cell survival and enhances HIF-1 transcriptional activity during hypoxia. *Cancer Res* **66**:6683–6691.

Kam AY, Chan AS, and Wong YH (2003) Rac and Cdc42-dependent regulation of c-Jun N-terminal kinases by the delta-opioid receptor. *J Neurochem* **84**: 503–513.

Kamiyama M, Pozzi A, Yang L, DeBusk LM, Breyer RM, and Lin PC (2006) EP2, a receptor for PGE2, regulates tumor angiogenesis through direct effects on endothelial cell motility and survival. *Oncogene* **25**:7019–7028.

Khan SM, Sleno R, Gora S, Zylbergold P, Laverdure JP, Labbé JC, Miller GJ, and Hébert TE (2013) The expanding roles of Gβγ subunits in G protein-coupled receptor signaling and drug action. *Pharmacol Rev* **65**:545–577.

Kharmate G, Rajput PS, Lin YC, and Kumar U (2013) Inhibition of tumor promoting signals by activation of SSTR2 and opioid receptors in human breast cancer cells. *Cancer Cell Int* **13**:93.
Kieffer BL and Evans CJ (2009) Opioid receptors: from binding sites to visible molecules in vivo. *Neuropharmacology* **56** (Suppl 1):205–212.
Kietzmann T, Mennerich D, and Dimova EY (2016) Hypoxia-inducible factors (HIFs) and phosphorylation: impact on stability, localization, and transactivity. *Front Cell Dev Biol* **4**:11.
Kodani E, Xuan YT, Shinmura K, Takano H, Tang XL, and Bolli R (2002) Delta-opioid receptor-induced late preconditioning is mediated by cyclooxygenase-2 in conscious rabbits. *Am J Physiol Heart Circ Physiol* **283**:H1943–H1957.
Kohutek ZA, diPierro CG, Redpath GT, and Hussaini IM (2009) ADAM-10-mediated N-cadherin cleavage is protein kinase C-α dependent and promotes glioblastoma cell migration. *J Neurosci* **29**:4605–4615.
Kong D, Park E J, Stephen A G, Calvani M, Cardellina J H, Monks A, Fisher R J, Shoemaker R H, Melillo G, et al. (2005) Echinomycin, a small-molecule inhibitor of hypoxia-inducible factor-1 DNA-binding activity. *Cancer Res* **65**:9047–9055.
Krock BL, Skuli N, and Simon MC (2011) Hypoxia-induced angiogenesis: good and evil. *Genes Cancer* **2**:1117–1133.
Leaney JL and Tinker A (2000) The role of members of the pertussis toxin-sensitive family of G proteins in coupling receptors to the activation of the G protein-gated inwardly rectifying potassium channel. *Proc Natl Acad Sci USA* **97**:5651–5656.
Livak KJ and Schmittgen TD (2001) Analysis of relative gene expression data using real-time quantitative PCR and the 2(-Delta Delta C(T)) method. *Methods* **25**: 402–408.
Martín M, Chan A, Dirix L, O'Shaughnessy J, Hegg R, Manikhas A, Shtivelband M, Krivorotko P, Batista López N, Campone M, et al. (2017) A randomized adaptive phase II/III study of buparlisib, a pan-class I PI3K inhibitor, combined with paclitaxel for the treatment of HER2- advanced breast cancer (BELLE-4). *Ann Oncol* **28**:313–320.
Pagé EL, Robitaille GA, Pouysségur J, and Richard DE (2002) Induction of hypoxia-inducible factor-1α by transcriptional and translational mechanisms. *J Biol Chem* **277**:48403–48409.
Pathan H and Williams J (2012) Basic opioid pharmacology: an update. *Br J Pain* **6**: 11–16.
Portoghese PS, Sultana M, and Takemori AE (1988) Naltrindole, a highly selective and potent non-peptide delta opioid receptor antagonist. *Eur J Pharmacol* **146**: 185–186.
Powis G, Bonjouklian R, Berggren MM, Gallegos A, Abraham R, Ashendel C, Zalkow L, Matter WF, Dodge J, Grindey G, et al. (1994) Wortmannin, a potent and selective inhibitor of phosphatidylinositol-3-kinase. *Cancer Res* **54**:2419–2423.
Riedl A, Schlederer M, Pudelko K, Stadler M, Walter S, Unterleuthner D, Unger C, Kramer N, Hengstschläger M, Kenner L, et al. (2017) Comparison of cancer cells in 2D vs 3D culture reveals differences in AKT-mTOR-S6K signaling and drug responses. *J Cell Sci* **130**:203–218.
Rodon J, Pérez-Fidalgo A, Krop IE, Burris H, Guerrero-Zotano G, Britten CD, Becerra C, Schellens J, Richards DA, Schuler M, et al. (2018) Phase 1/1b dose escalation and expansion study of BEZ235, a dual PI3K/mTOR inhibitor, in patients with advanced solid tumors including patients with advanced breast cancer. *Cancer Chemother Pharmacol* **82**:285–298.
Rouillard AD, Gundersen GW, Fernandez NF, Wang Z, Monteiro CD, McDermott MG, and Ma'ayan A (2016) The harmonizome: a collection of processed datasets gathered to serve and mine knowledge about genes and proteins. *Database (Oxford)* **2016**:1–16.
Rozic JG, Chakraborty C, and Lala PK (2001) Cyclooxygenase inhibitors retard murine mammary tumor progression by reducing tumor cell migration, invasiveness and angiogenesis. *Int J Cancer* **93**:497–506.
Ruohola JK, Valve EM, Karkkainen MJ, Joukov V, Alitalo K, and Härkönen PL (1999) Vascular endothelial growth factors are differentially regulated by steroid hormones and antiestrogens in breast cancer cells. *Mol Cell Endocrinol* **149**:29–40.
Satoh M and Minami M (1995) Molecular pharmacology of the opioid receptors. *Pharmacol Ther* **68**:343–364.
Schofield CJ and Ratcliffe PJ (2004) Oxygen sensing by HIF hydroxylases. *Nat Rev Mol Cell Biol* **5**:343–354.
Schwab LP, Peacock DL, Majumdar D, Ingels JF, Jensen LC, Smith KD, Cushing RC, and Seagroves TN (2012) Hypoxia-inducible factor 1α promotes primary tumor growth and tumor-initiating cell activity in breast cancer. *Breast Cancer Res* **14**:R6.
Shadeo A and Lam WL (2006) Comprehensive copy number profiles of breast cancer cell model genomes. *Breast Cancer Res* **8**:R9.
Smith P, Rhodes NP, Ke Y, and Foster CS (2002) Upregulation of estrogen and androgen receptors modulate expression of FGF-2 and FGF-7 in human, cultured, prostatic stromal cells exposed to high concentrations of estradiol. *Prostate Cancer Prostatic Dis* **5**:105–110.
St-Germain ME, Gagnon V, Parent S, and Asselin E (2004) Regulation of COX-2 protein expression by Akt in endometrial cancer cells is mediated through NF-kappaB/IkappaB pathway. *Mol Cancer* **3**:7.
Vlahos CJ, Matter WF, Hui KY, and Brown RF (1994) A specific inhibitor of phosphatidylinositol 3-kinase, 2-(4-morpholinyl)-8-phenyl-4H-1-benzopyran-4-one (LY294002). *J Biol Chem* **269**:5241–5248.
Vojdani A, Choppa PC, Tagle C, Andrin R, Samimi B, and Lapp CW (1998) Detection of Mycoplasma genus and Mycoplasma fermentans by PCR in patients with chronic fatigue syndrome. *FEMS Immunol Med Microbiol* **22**:355–365.
Wang D and Dubois RN (2004) Cyclooxygenase-2: a potential target in breast cancer. *Semin Oncol* **31** (1 Suppl 3):64–73.
Warfel NA, Dolloff NG, Dicker DT, Malysz J, and El-Deiry WS (2013) CDK1 stabilizes HIF-1α via direct phosphorylation of Ser668 to promote tumor growth. *Cell Cycle* **12**:3689–3701.
Wei YC, Zhang B, Li X, Liu XM, Zhang J, Lei B, Li B, Zhai R, Chen Q, and Li Y (2016) Upregulation and activation of δ-opioid receptors promotes the progression of human breast cancer. *Oncol Rep* **36**:2579–2586.
World Health Organization (WHO) (1996) *Cancer Pain Relief: With a Guide to Opioid Availability*, World Health Organization, Geneva, Switzerland.
Xia S, Zhao Y, Yu S, and Zhang M (2010) Activated PI3K/Akt/COX-2 pathway induces resistance to radiation in human cervical cancer HeLa cells. *Cancer Biother Radiopharm* **25**:317–323.
Yamashita K, Discher DJ, Hu J, Bishopric NH, and Webster KA (2001) Molecular regulation of the endothelin-1 gene by hypoxia. Contributions of hypoxia-inducible factor-1, activator protein-1, GATA-2, AND p300/CBP. *J Biol Chem* **276**: 12645–12653.
Yang D, Tian HY, Zang TN, Li M, Zhou Y, and Zhang JF (2017) Hypoxia imaging in cells and tumor tissues using a highly selective fluorescent nitroreductase probe. *Sci Rep* **7**:9174.
Yoon SH, Jin W, Spencer RJ, Loh HH, and Thayer SA (1998) Desensitization of delta-opioid-induced mobilization of Ca2+ stores in NG108-15 cells. *Brain Res* **802**:9–18.
Yu S, Kim T, Yoo KH, and Kang K (2017) The T47D cell line is an ideal experimental model to elucidate the progesterone-specific effects of a luminal A subtype of breast cancer. *Biochem Biophys Res Commun* **486**:752–758.
Yuan Y, Hilliard G, Ferguson T, and Millhorn DE (2003) Cobalt inhibits the interaction between hypoxia-inducible factor-alpha and von Hippel-Lindau protein by direct binding to hypoxia-inducible factor-alpha. *J Biol Chem* **278**:15911–15916.
Zagon IS, McLaughlin PJ, Goodman SR, and Rhodes RE (1987) Opioid receptors and endogenous opioids in diverse human and animal cancers. *J Natl Cancer Inst* **79**: 1059–1065.
Zhang Z, Xin SM, Wu GX, Zhang WB, Ma L, and Pei G (1999) Endogenous δ-opioid and ORL1 receptors couple to phosphorylation and activation of p38 MAPK in NG108-15 cells and this is regulated by protein kinase A and protein kinase C. *J Neurochem* **73**:1502–1509.
Zhong H, Chiles K, Feldser D, Laughner E, Hanrahan C, Georgescu MM, Simons JW, and Semenza GL (2000) Modulation of hypoxia-inducible factor 1α expression by the epidermal growth factor/phosphatidylinositol 3-kinase/PTEN/AKT/FRAP pathway in human prostate cancer cells: implications for tumor angiogenesis and therapeutics. *Cancer Res* **60**:1541–1545.
Zhong H, De Marzo AM, Laughner E, Lim M, Hilton DA, Zagzag D, Buechler P, Isaacs WB, Semenza GL, and Simons JW (1999) Overexpression of hypoxia-inducible factor 1alpha in common human cancers and their metastases. *Cancer Res* **59**:5830–5835.
Zundel W, Schindler C, Haas-Kogan D, Koong A, Kaper F, Chen E, Gottschalk AR, Ryan HE, Johnson RS, Jefferson AB, et al. (2000) Loss of PTEN facilitates HIF-1-mediated gene expression. *Genes Dev* **14**:391–396.

Address correspondence to: Daniela A. Fux, University of Veterinary Medicine Vienna, Veterinaerplatz 1, 1210 Vienna, Austria. E-mail: daniela.fux@vetmeduni.ac.at

Alexandra Schoos, Cordula Gabriel, Vanessa M. Knab, Daniela A. Fux

Activation of HIF-1α by δ-opioid receptors in breast cancer cells induces COX-2 expression for paracrine activation of vascular endothelial cells

The Journal of Pharmacology and Experimental Therapeutics

Supplemental Figures

Fig. 1

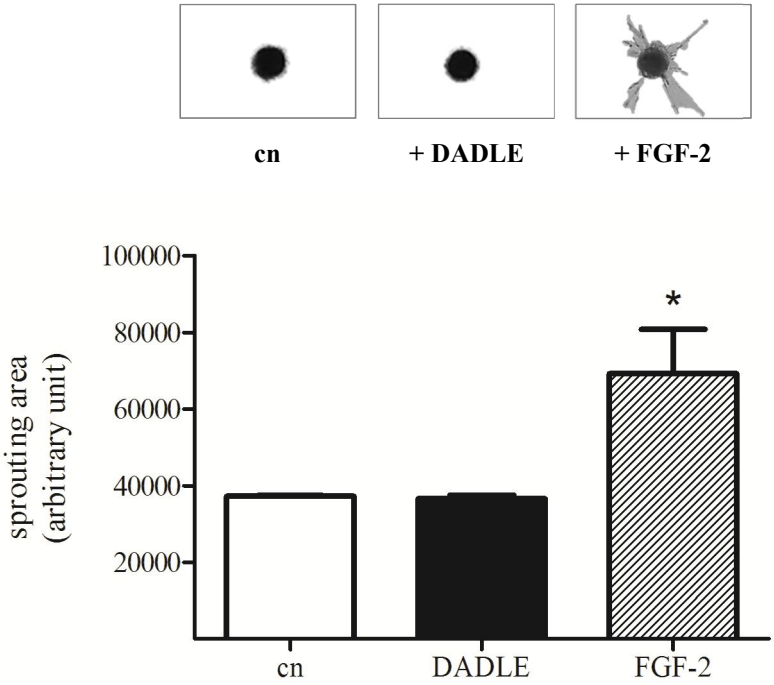

END cell spheroids were exposed to 1 μM DADLE and examined for sprout formation after 5 days. Negative controls (cn) remained untreated. For positive sprouting control, spheroids were treated with 20 ng/ml FGF-2 for 24 h. Pictures show representative spheroids. Sprouting area was determined from 6-8 randomly selected spheroids per experimental group and expressed as mean ± SEM. * $p < 0.05$ compared to non-treated controls (cn) by unpaired Welch's t-test.

Fig. 2

A

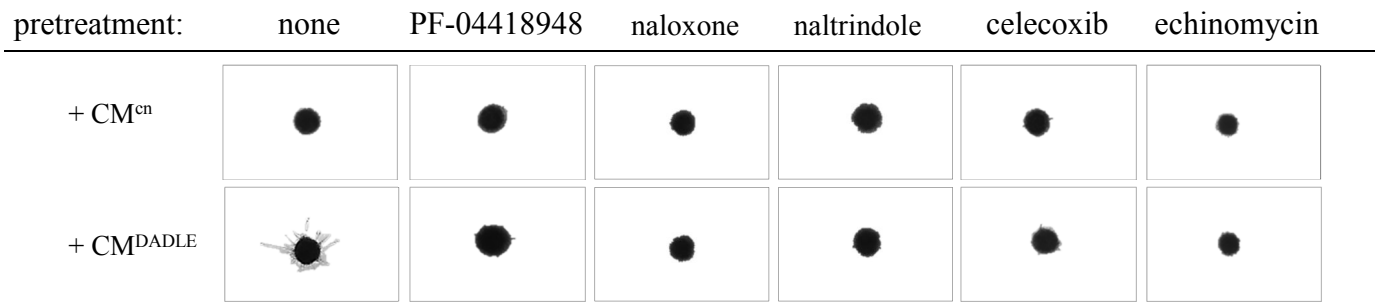

B

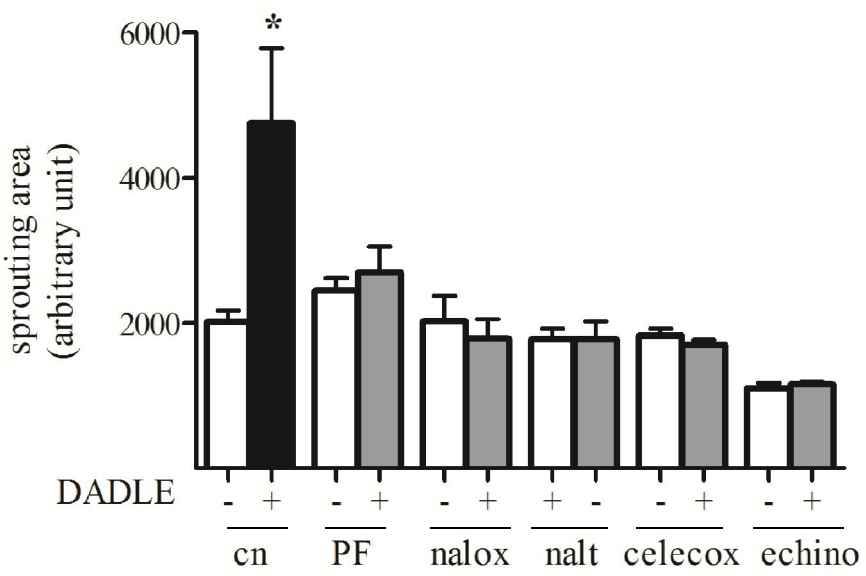

A) END cells were exposed to CM obtained from T47D cells treated with 1 µM DADLE alone (CM^{DADLE}) or together with 10 µM naloxone (nalox), 10 µM naltrindole (nalt), 10 nM echinomycin ($CM^{echino/DA}$) or 50 µM celecoxib ($CM^{cele/DA}$). CM collected from non-treated T47D cells served as control (CM^{cn}). In addition, END cells were treated with 10 µM PF-04418948 (PF) for 30 min before being exposed to CM^{DADLE}. Pictures show representatives END cell spheroids from each treatment group after 5 day-incubation. B) Quantification of sprouting areas. Sprouting area was determined from 6-10 randomly selected spheroids per experimental group from three independent experiments and presented as mean ± SEM. * $p < 0.05$ compared to CM^{cn} by unpaired Welch's t-test.